




## Article

# Cd Removal from Aqueous Solutions Using a New Modified Zeolite Adsorbent

He Zhang, Shuo Gao, Xiaoxu Cao, Jitong Lin, Jingyi Feng, Hui Wang, Hong Pan , Quangang Yang, Yanhong Lou  and Yuping Zhuge 

National Engineering Research Center for Efficient Utilization of Soil and Fertilizer Resources, College of Resources and Environment, Shandong Agricultural University, Tai'an 271018, China  
\* Correspondence: yanhonglou1985@163.com (Y.L.); zhugeyp@sdau.edu.cn (Y.Z.)

**Abstract:** Water cadmium (Cd) pollution has widely aroused concerns due to high Cd toxicity in water bodies and its serious health risks to humans. Adsorption has been identified as an effective and widely utilized technology for water purification with heavy metal pollution. To develop a newly identified adsorbent of modified zeolite that can easily and effectively purify Cd-polluted water, NaOH modification (JZ), high-temperature modification (HZ), humic acid modification (FZ), Na<sub>2</sub>S modification (SZ), and ultrasonic modification (CZ) zeolites were developed, and their appearances and adsorption and desorption characteristics were investigated. The results showed that the adsorption capacity of Cd by JZ and SZ were improved by 68.87% and 32.06%, respectively, relative to that by natural zeolite (NZ); however, HZ, FZ, and CZ decreased the adsorption capacity. JZ had a higher adsorption capacity than SZ and could remove 99.90% Cd at an initial concentration of 100 mg/L. The dominant adsorption mechanism of Cd by JZ was the chemisorption of the monolayer. The preferred temperature and pH that enhanced Cd adsorption by JZ were 25–35 °C and 4–8, respectively. With an equilibrium adsorption capacity of 9.37–9.74 mg/g at an initial concentration of 280 mg/L, JZ reached its maximum saturated adsorption capacity; compared with SZ and NZ, the adsorption capacity increase was 27.83–68.81%. The R<sup>2</sup> fitted by JZ's Langmuir model and quasi-second-order dynamics model were both above 0.93. In summary, JZ was recognized as a novel adsorbent for Cd-polluted water purification.

**Keywords:** modified zeolite; cadmium pollution; adsorption; desorption



**Citation:** Zhang, H.; Gao, S.; Cao, X.; Lin, J.; Feng, J.; Wang, H.; Pan, H.; Yang, Q.; Lou, Y.; Zhuge, Y.

Cd Removal from Aqueous Solutions Using a New Modified Zeolite Adsorbent. *Minerals* **2023**, *13*, 197. <https://doi.org/10.3390/min13020197>

Academic Editors: Nikolaos Kantiranis, Anestis A. Filippidis and Chiharu Tokoro

Received: 30 November 2022

Revised: 21 January 2023

Accepted: 28 January 2023

Published: 29 January 2023



**Copyright:** © 2023 by the authors. Licensee MDPI, Basel, Switzerland. This article is an open access article distributed under the terms and conditions of the Creative Commons Attribution (CC BY) license (<https://creativecommons.org/licenses/by/4.0/>).

## 1. Introduction

Water polluted by heavy metal is recognized as an environmental problem attributed to the emission of waste residue, water, and gas [1]. Cadmium (Cd), one of the most toxic metals, has been recognized as a carcinogenic agent; excess Cd accumulated in water systems is harmful to the survival and reproduction of algae, insects, fish, and other aquatic life [2]. Many studies have indicated that a series of physiological disorders experienced by aquatic organisms that were exposed to Cd regimes, such as water body pollution, destroying the biodiversity of aquatic systems by reducing the reproduction rate of the aquatic organisms, which may lead to low population levels or extinction of many freshwater species [3,4]. Furthermore, Cd can enter the body and accumulated in organs through the food chain, causing health problems [5]. In addition to this, a detrimental threat is also posed to human health due to the long-term consumption of Cd-contaminated water, and causes serious harm to the kidney [6], liver [7], intestines, and stomach [8], leading to bone softening, kidney damage, bone pain, cancer [9–11], damage to the functional organs, and even death in severe cases. Therefore, it is imperative to control and purify heavy metal pollution in water.

To date, many methods, including ion exchange [12], chemical precipitation [13], membrane filtration [14], and adsorption [15], have been utilized to treat industrial and mining

wastewater with heavy metal pollution. Notably, adsorption was recognized as an effective and the most widely utilized technology for the purification of heavy metal-polluted water [16]. The key factor in the adsorption process is the selection of the adsorption materials. At present, natural and synthetic zeolite [17,18], biochar [19], and composite materials [20] are mainly used for the adsorption of heavy metals in wastewater. Among them is zeolite, a type of natural mineral that has high reserves in China, with a large specific surface area, increased pore size, and a rich cationic skeleton structure. Zeolite has good ion exchange ability and environmental compatibility and is often used to treat heavy metal-polluted wastewater [21]. Moreover, due to the presence of micro-sized holes in zeolite, molecular shape selectivity, specificity, and chemical and thermal stability (hydrothermal) are increased; therefore, zeolite has great potential and efficiency for pollutant adsorption and is receiving an increasing amount of attention worldwide [22,23].

However, the utilization of zeolite is restricted based on its intrinsic adsorption ability, which has led to the rise of a new research topic on methods to increase this adsorption ability. Previous studies have documented some modifications enhanced the adsorption performance of zeolite. Abdellaoui et al. [24] indicated that the removal rate of Cd was improved from 13.13 to 35.65% via the application of sulfuric acid-modified zeolite. Wajima et al. [25] also reported that the addition of diatomite to NaOH solution increased the Si content to synthesize zeolites, and the ion exchange capacity was increased from 50 to 130 cmol/kg, performed at a high cation exchange capacity. Fan et al. [26] modified natural zeolite (NZ) with cetyltrimethylammonium bromide (HDTMA) and a hexamethylenetetramine solution and found that the adsorption capacity of  $\text{Cr}^{6+}$  increased from 2.95 to 5.43 mg/g under the same condition. Wang et al. [27] determined that the adsorption capacity of  $\text{Cu}^{2+}$  in a solution increased gradually that coupled with pH value increase by loading  $\text{SiO}_2$  onto zeolite. When the initial concentration of the solution was 50 mg/L, pH was 5, and the adsorbent amount was 1.0 g/L, the removal rate of  $\text{Cu}^{2+}$  could reach more than 75%. Rao et al. [28] compared the adsorption of Cd and  $\text{Zn}^{2+}$  in wastewater using 4A zeolite and bentonite and studied the effects of pH, time, and amount of adsorbent added on the adsorption of heavy metals. The results showed that under pH conditions of 6.0–6.5, both 4A zeolite and bentonite adsorbed Cd and Zn from wastewater in accordance with the Freundlich adsorption isotherm model and that the adsorption capacity of 4A zeolite on Cd and Zn was significantly greater than that of bentonite. Therefore, it was determined that the adsorption capacity is affected by the different modification methods applied to zeolite, raw materials, and the environment.

In this study, five types of modified zeolites based on solubility improve, surface area increase, and adsorption performance enhancement,  $\text{Na}_2\text{S}$  modification (SZ) and humic acid modification (FZ) that was newly developed and NaOH modification (JZ), high-temperature modification (HZ), and ultrasonic modification (CZ) as references were used, and the adsorption and desorption experiments of Cd were carried out with NZs as the control. The objectives of this study were (1) to reveal the structural characteristics of modified zeolite using scanning electron microscopy (SEM) and Fourier transform infrared spectroscopy (FTIR); (2) to study the adsorption and desorption characteristics of modified zeolite using adsorption kinetics, isothermal adsorption, and desorption experiments; (3) to reveal the influence of modified zeolite on the adsorption of heavy metals using different water pollution levels, pH, adsorption times, and other factors, as well as to clarify its favorable utilization scope. This study revealed a novel, modified zeolite for the highly efficient adsorption of Cd from polluted water and also provided a scientific basis for the remediation of Cd pollution in water. These findings can have a significant impact on the control of Cd pollution in water.

## 2. Materials and Methods

### 2.1. Experiment Materials

NZ used in the study was natural clinoptilolite, originated from Shijiazhuang Lingshou County, with a diameter of 200 mesh, moisture content of less than 6.5%, and impurity

content of less than 1.0%. The major constituents in NZ sample were SiO<sub>2</sub> (66.46%), Al<sub>2</sub>O<sub>3</sub> (12.31%), and Fe<sub>2</sub>O<sub>3</sub> (1.50%), and minor constituents contained CaO and K<sub>2</sub>O, etc. The cation exchange capacity was 191.13 cmol/kg and pH was 8.10.

The CdCl<sub>2</sub>·2.5H<sub>2</sub>O, sodium hydroxide, and sodium sulfide were analytically pure-grade compounds purchased from Tianjin Kemiou Chemical Reagent Co., Ltd. (Tianjin, China). The humic acid was provided by Shandong Nongda Fertilizer Co., Ltd. (Jinan, China).

## 2.2. Test Method

### 2.2.1. Preparation of Modified Zeolite

NaOH modification (JZ): We weighed 100 g of zeolite and placed it in a 2 L beaker. Thereafter, 1 L of 2 mol/L NaOH solution was added to the beaker, which was placed in a 60 °C water bath for 3 h; the contents of the mixture were stirred with a glass rod to make full contact between the zeolite and solution. Finally, the supernatant was poured out, and the remaining zeolite was washed with deionized water until the filtrate became neutral (pH = 7.0). It was then dried at 105 °C until a constant weight was achieved.

High-temperature modification (HZ): We weighed 100 g of zeolite and placed it in a 150 mL crucible, which was further transferred to a muffle furnace with a temperature of 450 °C for 7 h; thereafter the crucible was cooled to 25 ± 2 °C.

Na<sub>2</sub>S modification (SZ): We weighed 100 g of high-temperature modified zeolite and placed it in a 2 L beaker, to which 1 L of 5% Na<sub>2</sub>S solution was added. The beaker was placed in a 60 °C water bath for 12 h and stirred with a glass rod to make full contact between the zeolite and solution. Finally, the supernatant was poured out, and the remaining zeolite was washed with deionized water until the filtrate became neutral (pH = 7.0). It was then dried at 105 °C until a constant weight was achieved.

Ultrasonic modification (CZ): We weighed 100 g of zeolite and placed in a 2 L beaker, to which 1 L of deionized water was slowly added; it was then ultrasonified at a power of 160 W for 2 h, after pouring out the supernatant. The remaining zeolite was washed with deionized water repeatedly until the filtrate became neutral (pH = 7.0). It was then dried at 105 °C until a constant weight was achieved.

Humic acid modification (FZ): We washed 100 g of high-temperature modified zeolite and placed it in a 2 L beaker, to which 1 L of 300 mg/L humic acid solution was slowly added; the beaker was then placed in a 40 °C water bath for 4 h and constantly stirred with a glass rod to ensure complete contact between the zeolite and solution. Finally, the supernatant was poured out, and the remaining zeolite was washed repeatedly with deionized water until the filtrate became neutral (pH = 7.0). It was then dried at 105 °C until a constant weight was achieved.

### 2.2.2. Characterization of Modified Zeolite

Clay mineral analysis of original and modified samples using directional polymerization X-ray diffraction (XRD, Bruker D8 ADVANCE, Bruker, Karlsruhe, Germany). The distribution of functional groups was measured by Fourier transform infrared spectroscopy (FTIR, VERTE X70 FTIR, Bruker Corporation, Karlsruhe, Germany). The structural morphology of the sample surface was observed by scanning electron microscope (SEM, JSM-6360LV, JEOL, Akishima, Japan).

### 2.2.3. Isothermal Adsorption Equilibrium Test

Cd solutions with concentrations of 10, 40, 70, 100, and 130 mg/L were prepared using a standard solution (purchased from Gb (Beijing) Inspection and Certification Co., Ltd. (Beijing, China)); standard values: 1000 µg/mL, medium: c(HNO<sub>3</sub>) = 1.0 mol/L). Briefly, 0.5 g of zeolite was weighed and placed into a 50 mL centrifuge tube, to which 25 mL of a particular Cd solution was added. The tube was shaken at 220 rpm for 24 h at 25 °C using a constant temperature oscillator (Model: ZD-85A, Changzhou Guohua Electric Appliance Co., Ltd., Changzhou, China). The supernatant was poured out and filtered using a 0.45 µm filter. The Cd concentration in the filtrate was determined using inductively coupled plasma

optical emission spectrometry (ICP-OES; iCAP 7000, Thermo Fisher Scientific, Waltham, MA, USA). Finally, after evaluating the adsorption capacity of five types of modified zeolites, the two with the best adsorption capacity were selected for further study.

#### 2.2.4. Isothermal Adsorption and Modeling Analysis

For this purpose, 0.5 g of modified zeolite was weighed and placed into a 50 mL centrifuge tube, to which 25 mL of a particular Cd solution was added. The tube was shaken at 25 °C at a speed of 220 rpm for 24 h using a thermostatic oscillator. The Cd concentrations in the initial water solutions were 10, 40, 70, 100, 130, 160, 190, 220, 250, 280, and 310 mg/L. The supernatant was filtered with a 0.45 µm filter, and the concentration of Cd in the filtrate was determined using ICP-OES. Meanwhile, NZ was employed as the control and subjected to similar treatment.

The adsorption capacity of Cd by zeolite, per unit mass ( $q_e$ ), was calculated according to Equation (1), and the Freundlich and Langmuir models were used to fit  $C_e$  as  $x$ -axis and  $q_e$  as the  $y$ -axis (Equations (2) and (3)) [29].

$$q_e = (C_0 - C_e) V / m \quad (1)$$

$$\text{Freundlich model: } q_e = K_f C_e^{1/n} \quad (2)$$

$$\text{Langmuir model: } q_e = b C_e q_m / (1 + b C_e) \quad (3)$$

where  $q_e$  represents the adsorption capacity of Cd by modified zeolite and natural zeolite per unit mass, mg/g;  $C_0$  represents the initial concentration of Cd in the solution, mg/L;  $C_e$  represents the concentration of Cd at adsorption equilibrium, mg/L;  $V$  represents the adsorption equilibrium of the solution volume, L;  $m$  represents the amount of zeolite added, g;  $K_f$  and  $n$  represent the empirical coefficients of Freundlich model; the greater the value of  $n$ , the better the adsorption performance.  $b$  is the adsorption equilibrium constant, L/g; the larger the value of  $b$ , the better the adsorption performance;  $q_m$  is the maximum adsorption capacity of a single molecular layer, mg/g.

#### 2.2.5. Isothermal Desorption

The isothermally adsorbed modified zeolites were washed twice with saturated sodium chloride, and thereafter, 50 mL of 0.01 mol/L potassium nitrate solution was added to it. The concentration of Cd in the filtrate was determined using ICP-OES.

The desorption effect was calculated using the following formula (Equation (4)):

$$\text{Desorption rate} = [C_2 / (C_0 - C_1)] \times 100\% \quad (4)$$

where  $C_0$  and  $C_1$ , respectively, represent the concentration of Cd in the solution before and after adsorption, mg/L, and  $C_2$  represents the desorption capacity of Cd, mg/L.

#### 2.2.6. Kinetics of the Reaction

For this purpose, 0.5 g of modified zeolites were weighed and added into a 50 mL centrifuge tube, to which 25 mL of 40 mg/L Cd solution was added at 25 °C and shaken (220 rpm). The concentration of Cd in the filtrate was determined at 10, 20, 40, 60, 80, and 120 min and 4, 6, 12, and 24 h using ICP-OES. The kinetic characteristics of Cd adsorption on the zeolite surface were analyzed by fitting the experimental data to the following three equations (Equations (5)–(7)):

$$\text{Quasi-first-order kinetic equation: } q_t = q_{e1} (1 - e^{-k_1 t_1}) \quad (5)$$

$$\text{Quasi-second-order dynamics equations: } q_t = k_2 q_{e2}^2 t_1 / (1 + k_2 q_{e2} t_1) \quad (6)$$

$$\text{Intraparticle diffusion model: } q_t = K_{id} t_2^{1/2} + C \quad (7)$$

where  $q_t$  is the adsorption capacity of the three zeolites to Cd at time  $t$ , mg/g;  $t_1$  is time of the adsorption reaction, h;  $q_{e1}$  is the theoretical adsorption capacity of Cd by zeolite at the adsorption equilibrium, obtained by fitting the quasi-first-order adsorption kinetics equation, mg/g;  $k_1$  is the first-order adsorption rate constant, /h;  $q_{e2}$  is the theoretical adsorption capacity of Cd by zeolite when the adsorption equilibrium is reached by fitting the quasi-second-order adsorption kinetic equation, mg/g;  $k_2$  is the second-order adsorption rate constant, g/(mg·h);  $K_{id}$  is the diffusion rate constant mg/(g·h<sup>0.5</sup>);  $t_2$  is the diffusion time, h;  $C$  is a constant (mg/g).

### 2.2.7. Effect of Initial pH of Solution on Cd Adsorption by Zeolite

A series of 50 mL centrifuge tubes were taken, to which 0.5 g of zeolite and 25 mL of Cd solutions, with an initial concentration of 40 mg/L and different initial pH values, (adjust pH to 2, 4, 6, and 8 with 1 mol/L HCl and NaOH solutions) were added successively; the tubes were shaken at a speed of 220 rpm at 25 °C for 24 h. These reaction solutions were stewed for 30 min. The concentration of Cd in the filtered supernatant was measured.

### 2.2.8. Effect of Temperature on the Adsorption Properties of Zeolite

A series of 50 mL centrifuge tubes were taken, to which 0.5 g of zeolite and 25 mL of Cd solutions were added. The Cd concentrations of the initial water solutions were 10, 40, 70, 100, 130, 160, and 190 mg/L, with a pH of 7. The samples were placed in a constant temperature oscillator (15, 25, and 35 °C, at a speed of 220 rpm) for 24 h. The reaction solutions were stewed for 30 min, and the supernatant was filtered using a 0.45 µm filter. The concentration of Cd in the filtrate was determined via ICP-OES using unmodified zeolite as the control.

## 2.3. Statistical Analysis

All the data were expressed as the mean value of the triplicate experiments, and data were analyzed using a one-way analysis of variance with the SPSS 19.0 software (SPSS Inc., Chicago, IL, USA), and the images were drawn using the Origin 2018 software (Origin Lab., Northampton, MA, USA).

## 3. Results

### 3.1. Characterization of Zeolite

The modified zeolite has no new substance formation, only the intensity of each characteristic diffraction peak has changed (based on the X-ray powder diffraction (XRPD) method). The crystallinity of each modified zeolite was significantly stronger than NZ at  $2\theta = 22.89^\circ$ , while the crystallinity of JZ and SZ were still significantly stronger than NZ at  $2\theta = 26.91^\circ$  and  $30.21^\circ$ , which may be due to the enhanced structural strength of zeolite by modification [30,31] (Figure 1). Four main adsorption peaks of nature and modified zeolites were detected in a wavenumber range of 450–1200 cm<sup>-1</sup> and stretching vibrations of Si–O–Mg at 456 cm<sup>-1</sup>, Si–O–Al at 992 cm<sup>-1</sup>, Si–O–Si at 1037 cm<sup>-1</sup>, and Si–O at 1182 cm<sup>-1</sup> (Figure 2) [32]. Compared to that in NZ, lower adsorption peaks were observed for Si–O–Si in JZ and SZ at 1037 cm<sup>-1</sup>. This phenomenon may be attributed to the existence of the OH<sup>-</sup>, which prevents the hydrolysis of the Si–O–Al bond [33]. However, the Si–O–Si bond is more likely to be broken by OH<sup>-</sup> in the absence of the Al tetrahedra. Therefore, the surface structure of JZ and SZ were more complex and loose, which consisted of a coral-like surface structure attributed to the desilicification that exposed to the alkali regime. A stretching vibration was detected in the adsorption peak of HZ at 3607 cm<sup>-1</sup> (O–H), and stronger adsorption peak in other modified zeolites, which may be caused due to the rupture of the O–H bond, leading to the loss of water molecules during the pyrolysis process, this is similar to the result of Ates A et al. [34] and Cardoso et al. [35], which make the O–H bond rupture. In addition to this, the adsorption peaks (the Si–O, Si–O–Al, and Si–O–Mg bonds were detected at 1182, 992, and 456 cm<sup>-1</sup>, respectively) of all the modified zeolites behaved in a similar waveform.

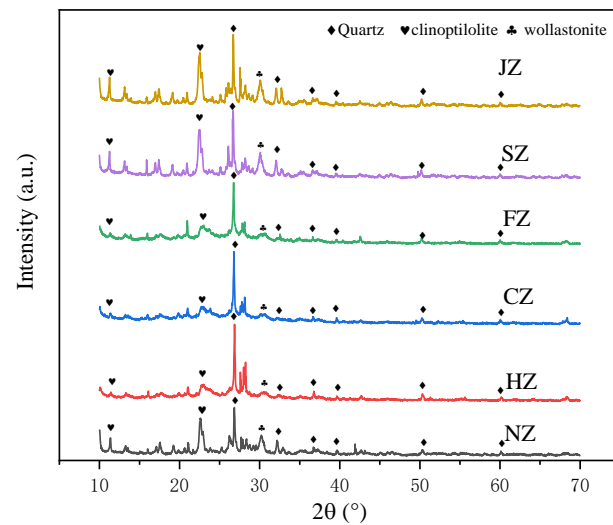


**Figure 1.** XRD patterns of zeolite. SZ:  $\text{Na}_2\text{S}$  modification; JZ: NaOH modification; CZ: ultrasonic modification; FZ: humic acid modification; HZ: high-temperature modification; NZ: natural zeolite.

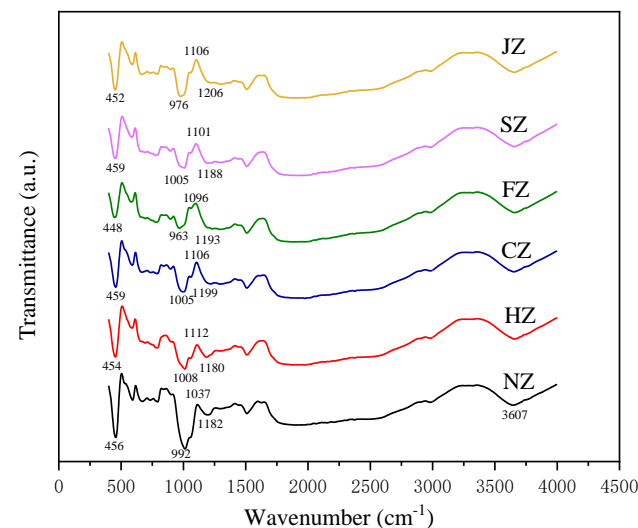


**Figure 2.** Fourier transform infrared spectroscopy results of zeolite. SZ:  $\text{Na}_2\text{S}$  modification; JZ: NaOH modification; CZ: ultrasonic modification; FZ: humic acid modification; HZ: high-temperature modification; NZ: natural zeolite.

Notably, compared to the surface smooth character of NZ, more coral-like structures were observed in JZ and SZ; this was a result of the corrosion caused by the alkali solutions, the results were consistent with the results of Murayama et al. [36] (Figure 3). Meanwhile, uneven surface structures were also detected in HZ and CZ, relative to NZ, due to material decomposition and water molecule evaporation inside the pores [37] because of high temperatures (HZ) as well as ultrasonic cavitation impurities in the zeolite pores (CZ) [38]. Furthermore, because the humic acid molecules [39] were attached to the surface of FZ, there were more raised bulges on its surface compared to that of NZ. The SEM images were consistent with the XRD results.

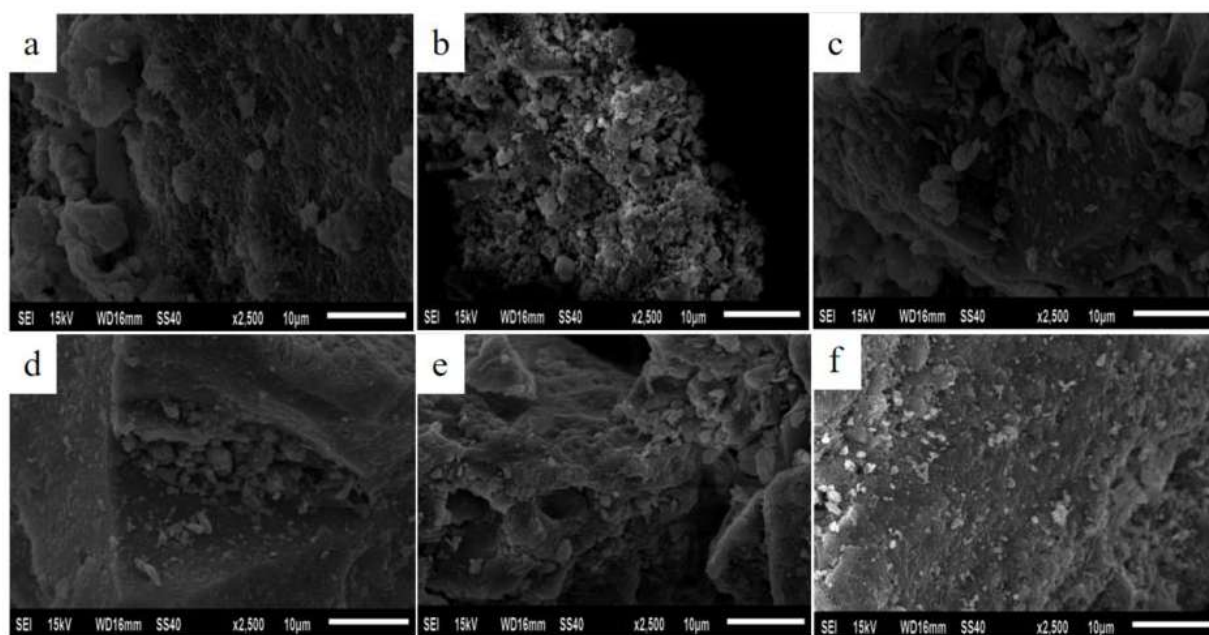


**Figure 3.** Scanning electron microscopic analysis of zeolite: (a) NaOH-modified zeolite, (b) Na<sub>2</sub>S-modified zeolite, (c) high temperature-modified zeolite, (d) humic acid-modified zeolite, (e) ultrasonic-modified zeolite, and (f) natural zeolite.

### 3.2. Isothermal Adsorption Characteristics of Modified Zeolite

The adsorption capacity of modified and unmodified zeolites was generally increased with an increase in the initial concentration of the Cd solutions; however, the concentrations at the equilibrium adsorption were different (Figure 4). Results showed that 99.90% and 93.44% of Cd, at an initial concentration of 100 mg/L, were adsorbed by JZ and SZ, respectively. Cd adsorption reached equilibrium at an initial concentration of 130 mg/L in CZ, with an equilibrium adsorption capacity of 3.97–4.43 mg/g. When the initial concentration was 250 mg/L, SZ, HZ, and FZ reached the maximum saturated adsorption capacity, with equilibrium adsorption capacities of 7.58–7.62, 4.78–5.18, and 4.52–4.93 mg/g, respectively. Furthermore, when the initial concentration was 280 mg/L, JZ reached the maximum saturated adsorption capacity, with an equilibrium adsorption capacity of 9.37–9.74 mg/g, compared with SZ and NZ, the adsorption capacity increase was 27.83–68.81%.

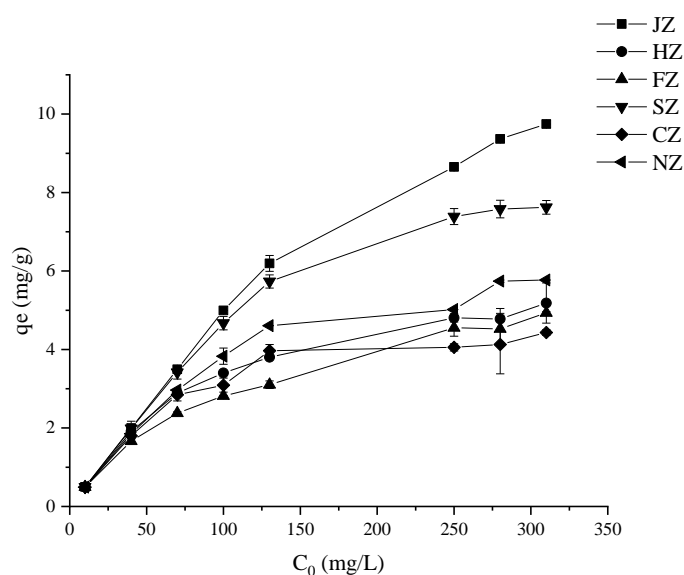


**Figure 4.** Curve presenting zeolite adsorption at different concentrations of Cd solution.

Compared to the Freundlich model, the Langmuir model can better describe the adsorption process of zeolite (Table 1, Figure 5). The results indicate that the adsorption of Cd by the three zeolites can be attributed to monolayer adsorption. Meanwhile, according to the Langmuir model nonlinear fitting data, the *b* of JZ (10.39) was higher than that of SZ (3.16), with a 69.59% increment, and the *b* of NZ was only 0.11. These results show the better spontaneous reaction and Cd adsorption capacity of JZ than that of SZ. Under the Langmuir model, the maximum saturated adsorption capacity of JZ and SZ were 1.75 and 1.09 times higher than that of NZ, respectively.

**Table 1.** Adsorption isothermal model parameters of modified and natural zeolite.

Isothermal Adsorption Model	NaOH Modification (JZ)	Na <sub>2</sub> S Modification (SZ)	Natural Zeolite (NZ)
Freundlich model	$k = 6.21 \pm 0.14$ $((\text{mg/g})/(\text{mg/L})^{1/n})$ $R^2 = 0.88$ $n = 10.52 \pm 1.05$	$k = 1.63 \pm 0.01$ $((\text{mg/g})/(\text{mg/L})^{1/n})$ $R^2 = 0.88$ $n = 3.02 \pm 0.15$	$k = 1.88 \pm 0.24$ $((\text{mg/g})/(\text{mg/L})^{1/n})$ $R^2 = 0.83$ $n = 4.64 \pm 0.77$
Langmuir model	$q_m = 9.74 \pm 0.38 \text{ mg/g}$ $R^2 = 0.96$ $b = 10.39 \pm 0.83 \text{ L/g}$	$q_m = 6.09 \pm 0.66 \text{ mg/g}$ $R^2 = 0.92$ $b = 3.16 \pm 0.37 \text{ L/g}$	$q_m = 5.58 \pm 0.13 \text{ mg/g}$ $R^2 = 0.98$ $b = 0.11 \pm 0.01 \text{ L/g}$

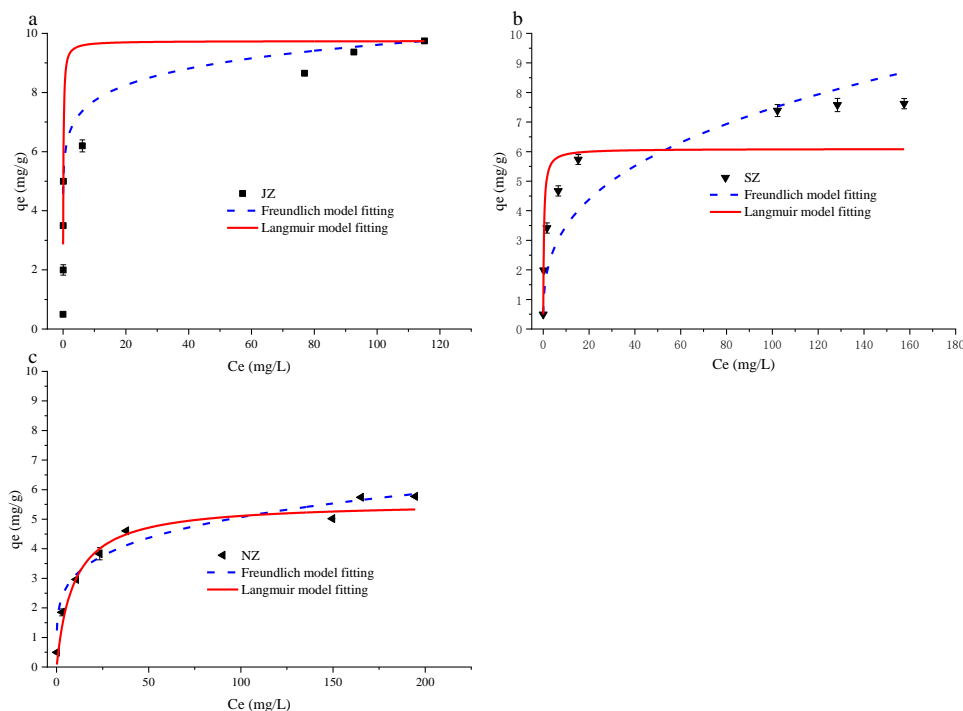


**Figure 5.** Adsorption isotherms of modified zeolites, (a) JZ and (b) SZ, and (c) natural zeolite (NZ).

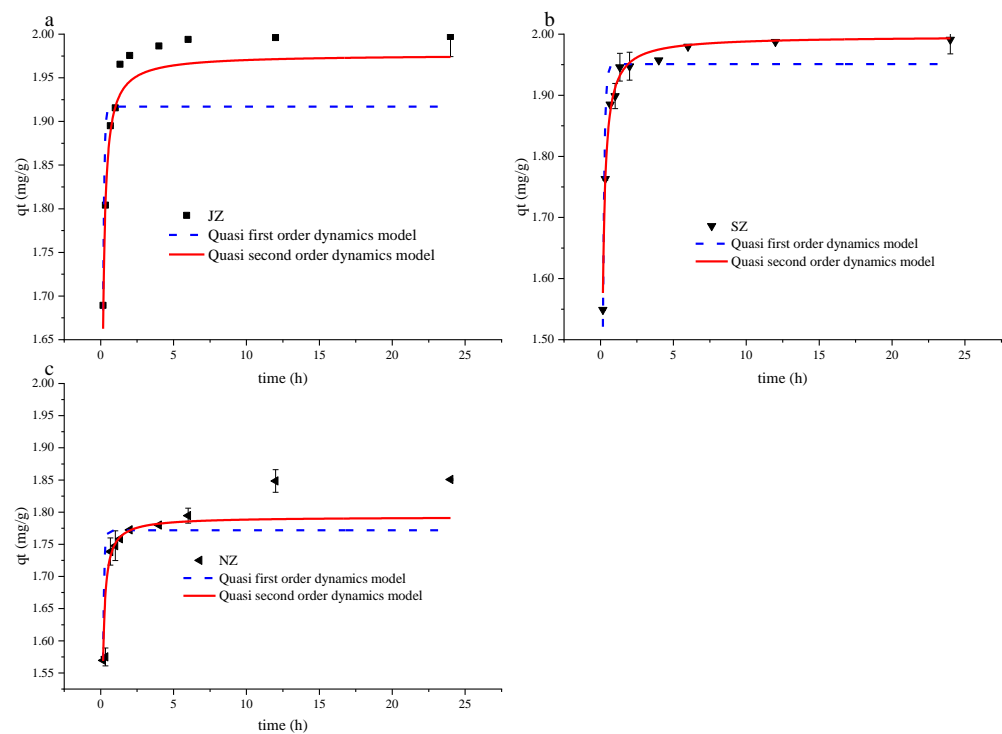
### 3.3. Adsorption Kinetics of Zeolite

Compared to the quasi-first-order kinetic model, the quasi-second-order kinetic model better describes the adsorption process of Cd in water by the modified and unmodified zeolites (Table 2, Figure 6). The maximum adsorption capacity of JZ and SZ according to the quasi-second-order kinetic model nonlinear fitting was similar to the measured value and higher than that of NZ, showing a 9.60% and 10.05% increment, respectively. These results indicate that this adsorption process was primarily controlled by chemical action.



**Table 2.** Adsorption kinetic equation parameters of modified and natural zeolite.

Adsorption Kinetic Model	NaOH Modification (JZ)	Na <sub>2</sub> S Modification (SZ)	Natural Zeolite (NZ)
Quasi-first-order dynamics model	$q_{e1} = 1.92 \text{ mg/g}$ $R^2 = 0.62$ $k_1 = 12.63 \pm 1.57 \text{ /h}$	$q_{e1} = 1.95 \text{ mg/g}$ $R^2 = 0.77$ $k_1 = 9.08 \pm 1.01 \text{ /h}$	$q_{e1} = 1.77 \text{ mg/g}$ $R^2 = 0.94$ $k_1 = 13.02 \pm 0.52 \text{ /h}$
Quasi-second-order dynamics model	$q_{e2} = 1.98 \text{ mg/g}$ $R^2 = 0.94$ $k_2 = 16.07 \pm 1.61 \text{ g/(mg}\cdot\text{h)}$	$q_{e2} = 1.99 \text{ mg/g}$ $R^2 = 0.96$ $k_2 = 11.27 \pm 0.55 \text{ g/(mg}\cdot\text{h)}$	$q_{e2} = 1.79 \text{ mg/g}$ $R^2 = 0.98$ $k_2 = 23.43 \pm 1.15 \text{ g/(mg}\cdot\text{h)}$

**Figure 6.** Adsorption kinetics of Cd by (a) JZ, (b) SZ, and (c) NZ.

Compared to that of NZ (80 min), the time of rapid adsorption stage of JZ (60 min) and SZ (60 min) was promoted by 25.00%, and the adsorption capacity was promoted by 10.53% and 9.64%, respectively (Figure 6). Additionally, NZ began to reach its adsorption equilibrium at 12 h, which was 6 h later than that for JZ (6 h) and SZ (6 h), and its equilibrium adsorption capacity was lower than that of JZ and SZ, with a 7.29–7.40% and 6.62–7.08% decrement, respectively.

The intraparticle diffusion model linear fitting indicated that the adsorption of Cd by JZ, SZ, and NZ was divided into three stages according to the adsorption kinetics (rapid adsorption, relative slow adsorption, and equilibrium adsorption; Figure 7). The order of the  $K$  values for each treatment (JZ, SZ, and NZ:  $K_1 > K_2 > K_3$ ) indicates that the adsorption rate of the liquid film diffusion during the early stages of adsorption was greater than that of the intraparticle diffusion during the middle and late stages (Table 3). Notably, the  $K$  value of the intraparticle diffusion model of JZ and SZ was significantly higher than that of NZ, increasing by 30.68–50.00% and 13.33–87.50%, respectively, which corresponded to the enhanced diffusion of JZ and SZ from the exterior surface of the adsorbent through the macropores and mesopores, respectively. However, because the graphs of the previous stages were not linear and did not pass through the origin, the intraparticle diffusion step was not considered the only rate-limiting step, this result is consistent with Cheung et al. [40].

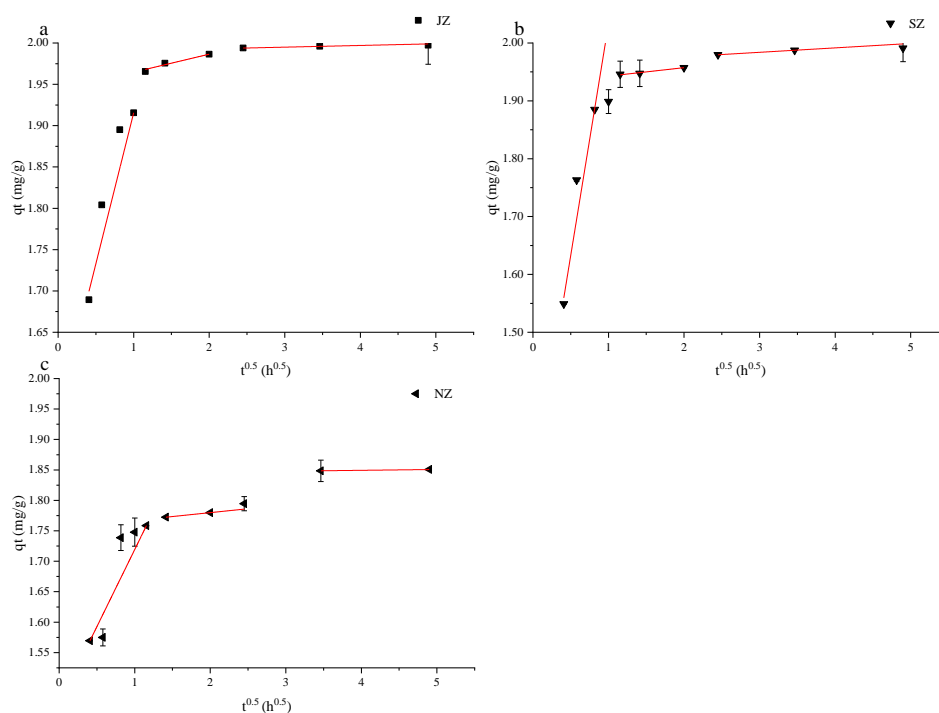


**Figure 7.** Fitting diagram of the Cd diffusion model by modified zeolites, (a) JZ and (b) SZ, and (c) natural zeolite (NZ).

**Table 3.** Fitting parameters of Cd diffusion in particles by modified zeolite.

Zeolite	$R_1^2$	$K_1$ (mg/g/h <sup>1/2</sup> )	$C_1$ (mg/g)	$R_2^2$	$K_2$ (mg/g/h <sup>1/2</sup> )	$C_2$ (mg/g)	$R_3^2$	$K_3$ (mg/g/h <sup>1/2</sup> )	$C_3$ (mg/g)
JZ	0.976	0.365	1.551	0.946	0.022	1.943	0.999	0.002	1.989
SZ	0.980	0.800	1.233	0.979	0.015	1.928	0.998	0.008	1.961
NZ	0.999	0.253	1.466	0.999	0.013	1.754	1.000	0.001	1.844

### 3.4. Effect of Initial Solution pH on Cd Adsorption by Zeolite

The pH of the solution has a sizable impact on the speciation of metal ions and the surface charge of the adsorbent [41]. The adsorption quantity was higher in JZ and SZ than in NZ (Figure 8). When the pH was 2, SZ and NZ had a similar adsorption capacity, whereas JZ had a higher adsorption capacity compared to SZ and NZ, by 75.00% and 73.61%, respectively. However, the adsorption capacity for SZ was significantly higher than that for NZ when the pH was 4, 6, and 8, and it increased by 46.38, 35.81, and 43.87%, respectively; meanwhile, the adsorption capacity for JZ was significantly higher than that for SZ and NZ, which increased by 22.61%–30.83% and 52.33%–63.16%, respectively. Notably, there was no significant difference in the adsorption capacities within the pH 4, 6, and 8 groups for each treatment (JZ, SZ, and NZ) and the lower adsorption capacity at pH 2 when compared to that at pH 4, 6, or 8. These results indicated that electrostatic interaction is the key mechanism of adsorption of Cd by JZ. The adsorption capacity of Cd is easily affected by the initial pH of the solution, which may be due to its small ionic radius [42].

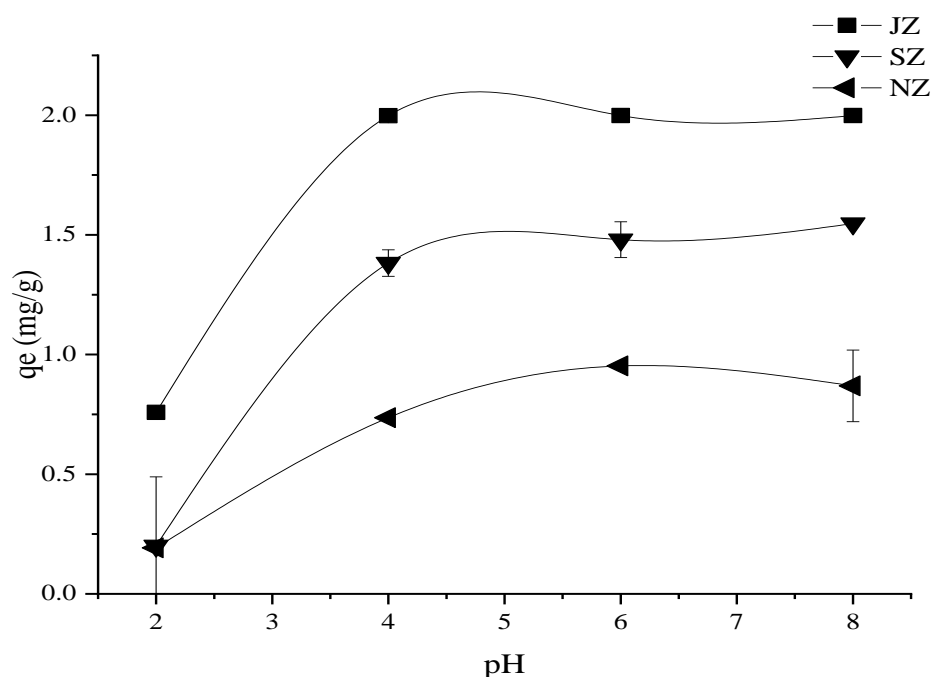


**Figure 8.** Effect of initial pH on Cd adsorption rate by different zeolites.

### 3.5. Influence of Temperature on the Adsorption Capacity of Zeolite

The effect of different temperatures on the adsorption of Cd for different modified zeolites varied (Figure 9). For JZ, when the initial concentration were 130, 160, and 190 mg/L, the adsorption capacity at 35 °C was significantly higher than that at 15 °C and 25 °C, with an increase of 5.60, 8.14, and 7.64% with respect to that at 15 °C and 5.43, 4.48, and 3.16% with respect to that at 25 °C; when the initial concentrations were 160 and 190 mg/L, the adsorption capacity at 25 °C was significantly higher than that at 15 °C by 3.86 and 4.62%, respectively. For SZ, when the initial concentrations were 130, 160, and 190 mg/L, the adsorption capacity at 35 °C was significantly higher than that at 15 °C by 4.15, 7.70, and 6.58%, respectively; when the initial concentrations were 130 and 160 mg/L, the adsorption capacity at 35 °C was significantly higher than that at 25 °C by 2.60 and 3.05%, respectively; when the initial concentrations were 130 and 160 mg/L, the adsorption capacity at 25 °C was significantly higher than at 15 °C by 1.44, and 5.04%, respectively. For NZ, when the initial concentrations were 100, 160, and 190 mg/L, the adsorption capacity at 35 °C was significantly higher than that at 15 °C by 4.07, 3.93, and 4.02%, respectively. However, the equilibrium adsorption capacities of JZ were significantly higher than that of SZ and NZ at temperatures between 15 and 35 °C and were increased by 7.98–8.95 and 28.49%–31.18%, respectively; meanwhile, the equilibrium adsorption capacities of SZ were significantly higher than that of NZ and were increased by 22.29, 23.29, and 24.42%, respectively.

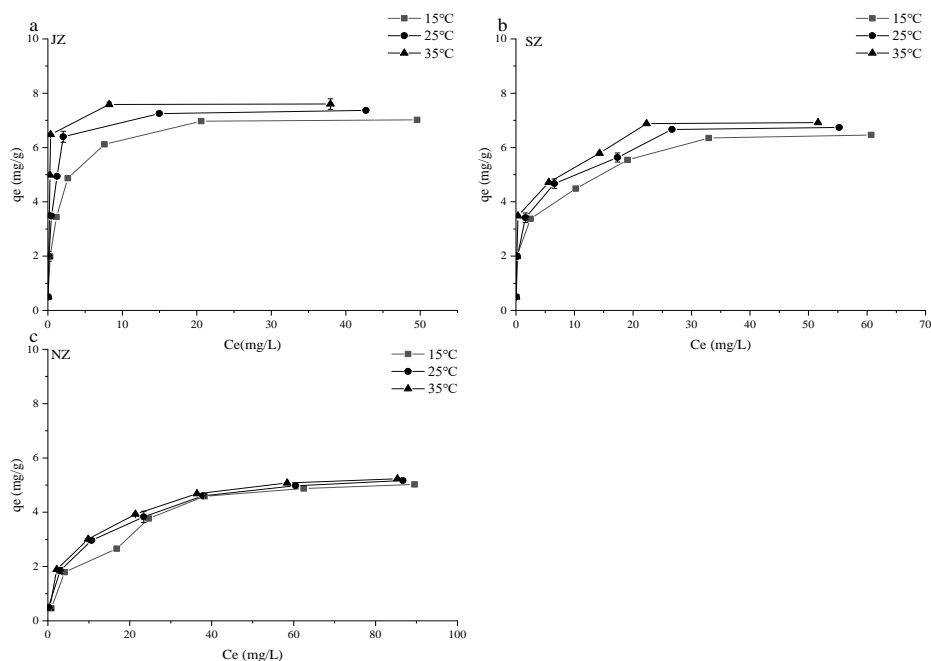


**Figure 9.** Adsorption curves of Cd for (a) JZ, (b) SZ, and (c) NZ at different temperatures (15, 25, and 35 °C).

**3.6. Desorption Characteristics of Modified Zeolite**

The effect of the initial concentration on Cd desorption from the different modified zeolites varied (Figure 10). With an increase in the initial concentration, the maximum desorption capacity of each treatment (JZ, SZ, and NZ) increased by 98.56, 99.48, and 98.15%, respectively; the desorption rate increased by 0.38, 5.78, and 25.20%, respectively (Table 4). Additionally, the maximum desorption capacity of SZ and NZ was 10.31 and 50.52 times higher than that of JZ. When the initial concentration of the solution was 130 mg/L, the desorption rate of SZ and NZ was significantly higher than that of JZ. The desorption rate of SZ was 13.22 times higher than that of JZ, and the desorption rate of NZ was 66.37 times higher than that of JZ and 5.02 times higher than that of SZ.

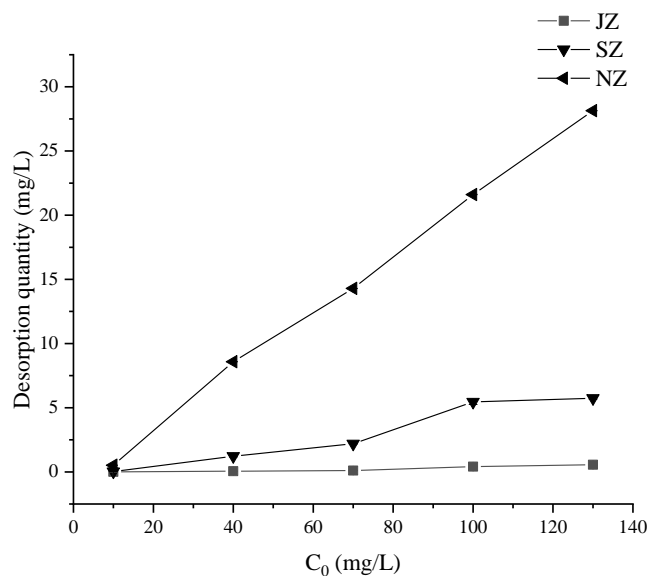


**Figure 10.** Curve presenting desorption of Cd by modified and natural zeolite.

**Table 4.** Desorption rates of Cd by modified and natural zeolite.

Initial Concentration (mg/L)	NaOH-Modified Zeolite (JZ,%)	Na <sub>2</sub> S-Modified Zeolite (SZ,%)	Natural Zeolite (NZ,%)
10	0.08 b	0.30 c	5.33 c
40	0.13 b	3.07 b	23.40 b
70	0.15 b	3.23 b	24.10 b
100	0.42 a	5.84 a	28.38 a
130	0.46 a	6.08 a	30.53 a

Note: the same letter in each column indicates no significant difference ( $p > 0.05$ ).

#### 4. Discussion

Adopting the adsorption method to purify heavy metal-polluted water is an economic and environmental approach, and selecting the most economically efficient adsorption material is an important factor for the adsorption process. Zeolite became an important adsorption material due to its large specific surface area and ion exchange properties, as well as its ability of not causing secondary pollution to the environment [43]. Moreover, the adsorption effect of zeolite can be further improved by modification, which will expand its application scope [44]. As Choi et al. [45] reported, Mg-zeolite successfully can adsorb >98% of the Pb, Cd, and Cu present in aqueous solutions. Qiu et al. [46] also indicated that polydopamine-modified zeolitic can remove 96% of Cd in a solution. Similar results were obtained in the present research, where 99.90 and 93.44% of the Cd were adsorbed by JZ and SZ at an initial concentration of 100 mg/L, respectively. This relatively high adsorption capacity of Cd by JZ and SZ may be attributed to their rough surface and coral-like structure, respectively, that increases the specific surface area via alkaline modification. Notably, the adsorption capacity of JZ was better than that of SZ; the maximum adsorption capacity of JZ (9.74 mg/g) was higher than that of SZ (7.62 mg/g), and the desorption capacity of JZ (0.46 mg/L) was lower than that of SZ (5.74 mg/L). Therefore, it could be concluded that compared to SZ, JZ is more efficient at Cd purification from water.

The Freundlich and Langmuir models were used to describe the process of adsorption. This study showed that the Langmuir model was more suitable to describe the adsorption isotherm; the results indicate that the adsorption of Cd by JZ and SZ followed monolayer adsorption on finite sites and uniform surfaces. This result was consistent with that of Han et al. [47], who revealed that the adsorption characteristics of manganese oxide-modified zeolite for Cd were in line with the Langmuir model and followed single molecular layer chemisorption. The quasi-first- and second-order kinetic models were used to describe the rate of the adsorption reaction. This study showed that the quasi-second-order dynamic model was more suitable for this research; the results indicated that the measured values of JZ and SZ were closer to the fitted values of the quasi-second-order kinetic model. The intraparticle diffusion model was used to describe the dynamics of the diffusion process within a particle. According to the intraparticle diffusion model, if the graph is linear and passes through the origin, the rate-limiting process will only have intraparticle diffusion [48]. However, this study showed that the intraparticle diffusion model of JZ and SZ had three phases: the first stage was mainly surface migration and diffusion; the second stage was mainly Cd diffusion into the cage structure through the pore structures; the third stage was mainly the completion of the intraparticle diffusion process. Since the graphs of the previous stages were not linear and did not pass through the origin, the intraparticle diffusion step was not considered to be the only rate-limiting step for JZ, SZ, and NZ. Peng et al. [49] studied the adsorption of heavy metal ions onto magnetic zeolite molecular sieves, and the graph of the intraparticle diffusion model showed a similar multistage pattern. Therefore, it can be concluded that the dominant adsorption mechanism of Cd by JZ and SZ is the chemisorption of the monolayer.

The right temperature and pH of the adsorbent material were necessary for it to work. Al-anber et al. [50] found that when the temperature rose from 20 to 30 °C, the removal rate of zeolite increased significantly. This study also found that the adsorption

of Cd by zeolite changed with temperature. JZ and SZ had better adsorption capacity at temperatures between 25 and 35 °C and lower adsorption capacity when the temperature was lower than 25 °C. This result is not consistent with the typical of an exothermic process that is characteristic of the physisorption phenomenon, this phenomenon may be attributed to the different material or the temperature range settings; Al-anber et al. [50] also found that the adsorption efficiency of Jordanian natural zeolite decreased when the temperature was 30–50 °C. The pH of the solution also significantly affects the surface charge of the adsorbent and the speciation of the metal ions [41,51,52]. The results from this study show that the adsorption process of JZ and SZ was significantly affected by the pH of the solution. A pH of 4–8 was favorable for adsorption; a strong acid inhibits the adsorption, whereas a weak base contributes to the adsorption. Zeolite will preferentially adsorb H<sup>+</sup> ions from an acidic solution; the H<sup>+</sup> ions compete with the Cd to occupy the Cd adsorption sites. Therefore, the metal adsorption efficiency depends on the pH of the solution. Moreno et al. [53] also found that a strongly acidic environment inhibits the adsorption of Cd by zeolite. Therefore, the preferred temperature and pH that enhanced Cd adsorption were determined to be between 25 and 35 °C and 4 and 8, respectively, for JZ and SZ. However, the adsorption capacity of other heavy metal ions or organic pollutant of JZ and SZ should be investigated in further study, and comparing the adsorption capacities of modified zeolite with other adsorption materials should also be focused.

## 5. Conclusions

An effective adsorption material, namely JZ, was developed in this study, that exhibited a favorable adsorption capacity for Cd. The dominant adsorption mechanism of Cd was the chemisorption of the monolayer. Furthermore, the preferred temperature and pH conditions that enhanced the adsorption of Cd by JZ were between 25 and 35 °C and 4 and 8, respectively. Future research should focus on comparing the adsorption capacities of JZ with other adsorption materials, as well as the adsorption efficiency on other organic and inorganic pollutant combinations.

**Author Contributions:** Data curation, H.Z., S.G., X.C. and J.L.; writing—original draft, H.Z.; formal analysis, H.Z., X.C., J.L., J.F., H.P. and Q.Y.; investigation, H.Z. and S.G.; methodology, J.F. and H.W.; software, H.W. and H.P.; resources, Q.Y.; conceptualization, Y.L. and Y.Z.; supervision, Y.L.; writing—review and editing, Y.L. and Y.Z.; funding acquisition, Y.Z.; project administration, Y.Z. All authors have read and agreed to the published version of the manuscript.

**Funding:** This work was supported by Major Science and Technology Innovation Projects in the Shandong Province (2021CXGC010804) and Natural Science Foundation of Shandong province (ZR2022MD073).

**Data Availability Statement:** The data provided in this study can be obtained at the request of the corresponding author.

**Conflicts of Interest:** The authors declare no conflict of interest.

## References

1. An, F.; Gao, B.; Dai, X.; Wang, M.; Wang, X. Efficient removal of heavy metal ions from aqueous solution using salicylic acid type chelate adsorbent. *J. Hazard. Mater.* **2011**, *192*, 956–962. [[CrossRef](#)] [[PubMed](#)]
2. Stankovic, S.; Kalaba, P.; Stankovic, A.R. Biota as toxic metal indicators. *Environ. Chem. Lett.* **2014**, *12*, 63–84. [[CrossRef](#)]
3. Closs, G.P.; Angermeier, P.L.; Darwall, W.R.; Balcombe, S.R. Why are freshwater fish so threatened. In *Conservation of Fresh Water Fishes*; Closs, G.P., Krkosek, M., Olden, J., Eds.; Cambridge University Press: Cambridge, UK, 2015; pp. 37–75.
4. Hamilton, P.B.; Cowx, I.G.; Oleksiak, M.F.; Griffiths, A.M.; Grah, M.; Stevens, J.R.; Carvalho, G.R.; Nicol, E.; Tyler, C.R. Population-level consequences for wild fish exposed to sublethal concentrations of chemicals—A critical review. *Fish Fish.* **2016**, *17*, 545–566. [[CrossRef](#)]
5. Zhang, H.; Reynolds, M. Cadmium exposure in living organisms: A short review. *Sci. Total Environ.* **2019**, *678*, 761–767. [[CrossRef](#)] [[PubMed](#)]
6. Orłowski, C.; Piotrowski, J.K. Biological levels of cadmium and zinc in the small intestine of non-occupationally exposed human subjects. *Hum. Exp. Toxicol.* **2003**, *22*, 57–63. [[CrossRef](#)] [[PubMed](#)]

7. Ya, J.; Xu, Y.; Wang, G.; Zhao, H. Cadmium induced skeletal underdevelopment, liver cell apoptosis and hepatic energy metabolism disorder in *Bufo gargarizans* larvae by disrupting thyroid hormone signaling. *Ecotoxicol. Environ. Saf.* **2021**, *211*, 111957. [[CrossRef](#)]
8. Nordberg, G.F. Cadmium and health in the 21st century—Historical remarks and trends for the future. *Biometals* **2004**, *17*, 485–489. [[CrossRef](#)]
9. Rinaldi, M.; Micali, A.; Marini, H.; Adamo, E.B.; Puzzolo, D.; Pisani, A.; Trichilo, V.; Altavilla, D.; Squadrito, F.; Minutoli, L. Cadmium, organ toxicity and therapeutic approaches: A review on brain, kidney and testis damage. *Curr. Med. Chem.* **2017**, *24*, 3879–3893. [[CrossRef](#)]
10. Ali, I.; Damdimopoulou, P.; Stenius, U.; Halldin, K. Cadmium at nanomolar concentrations activates Raf–MEK–ERK1/2 MAPKs signaling via EGFR in human cancer cell lines. *Chem.-Biol. Interact.* **2015**, *231*, 44–52. [[CrossRef](#)]
11. Kazantzis, G. Cadmium, osteoporosis and calcium metabolism. *Biometals* **2004**, *17*, 493–498. [[CrossRef](#)]
12. Kołodziejka, D.; Krukowska-Bak, J.; Kazmierczak-Razna, J.; Pietrzak, R. Uptake of heavy metal ions from aqueous solutions by sorbents obtained from the spent ion exchange resins. *Microporous. Mesoporous. Mater.* **2017**, *244*, 127–136. [[CrossRef](#)]
13. Wang, L.K.; Vaccari, D.A.; Li, Y.; Shamma, N.K. Chemical precipitation. In *Physicochemical Treatment Processes*; Humana Press: Totowa, NJ, USA, 2005; pp. 141–197.
14. Chowdhury, S.; Halder, G.; Mandal, T.; Sikder, J. Cetylpyridinium bromide assisted micellar-enhanced ultrafiltration for treating enrofloxacin-laden water. *Sci. Total Environ.* **2019**, *687*, 10–23. [[CrossRef](#)] [[PubMed](#)]
15. Bagheri, S.; Amini, M.M.; Behbahani, M.; Rabiee, G. Low cost thiol-functionalized mesoporous silica, KIT-6-SH, as a useful adsorbent for cadmium ions removal: A study on the adsorption isotherms and kinetics of KIT-6-SH. *Microchem. J.* **2019**, *145*, 460–469. [[CrossRef](#)]
16. Babel, S.; Kurniawan, T.A. Low-cost adsorbents for heavy metals uptake from contaminated water: A review. *J. Hazard. Mater.* **2003**, *97*, 219–243. [[CrossRef](#)]
17. Miandad, R.; Barakat, M.A.; Rehan, M.; Aburiazaiza, A.S.; Ismail, I.M.I.; Nizami, A.S. Plastic waste to liquid oil through catalytic pyrolysis using natural and synthetic zeolite catalysts. *Waste Manag.* **2017**, *69*, 66–78. [[CrossRef](#)]
18. Erdem, E.; Karapinar, N.; Donat, R. The removal of heavy metal cations by natural zeolites. *J. Colloid Interface Sci.* **2004**, *280*, 309–314. [[CrossRef](#)]
19. Wang, D.; Wang, D.; Yu, J.; Chen, Z.; Li, Y.; Gao, S. Role of alkali sodium on the catalytic performance of red mud during coal pyrolysis. *Fuel Process. Technol.* **2019**, *186*, 81–87. [[CrossRef](#)]
20. Lei, C.; Gao, J.; Ren, W.; Xie, Y.; Abdalkarim, S.Y.H.; Wang, S.; Ni, Q.; Yao, J. Fabrication of metal-organic frameworks@ cellulose aerogels composite materials for removal of heavy metal ions in water. *Carbohydr. Polym.* **2019**, *205*, 35–41. [[CrossRef](#)]
21. Visa, M. Synthesis and characterization of new zeolite materials obtained from fly ash for heavy metals removal in advanced wastewater treatment. *Powder Technol.* **2016**, *294*, 338–347. [[CrossRef](#)]
22. Jiang, N.; Shang, R.; Heijman, S.G.J.; Rietveld, L.C. High-silica zeolites for adsorption of organic micro-pollutants in water treatment: A review. *Water Res.* **2018**, *144*, 145–161. [[CrossRef](#)]
23. Aljerf, L. High-efficiency extraction of bromocresol purple dye and heavy metals as chromium from industrial effluent by adsorption onto a modified surface of zeolite: Kinetics and equilibrium study. *J. Environ. Manag.* **2018**, *225*, 120–132. [[CrossRef](#)]
24. Abdellaoui, Y.; Olguin, M.T.; Abatal, M.; Bassam, A.; Giacomán-Vallejo, G. Relationship between Si/Al ratio and the sorption of Cd (II) by natural and modified clinoptilolite-rich tuff with sulfuric acid. *Desalin. Water Treat.* **2019**, *150*, 157–165. [[CrossRef](#)]
25. Wajima, T.; Haga, M.; Kuzawa, K.; Ishimoto, H.; Tamada, O.; Ito, K.; Nishiyama, T.; Downs, R.T.; Rakovan, J.F. Zeolite synthesis from paper sludge ash at low temperature (90 °C) with addition of diatomite. *J. Hazard. Mater.* **2006**, *132*, 244–252. [[CrossRef](#)]
26. Fan, S.; Wang, C.; Feng, X. Adsorption of Cr<sup>6+</sup> from water by natural zeolite and modified zeolite. *Nonmet. Ores* **2006**, *29*, 56–57, (in Chinese with English abstract).
27. Wang, K.; Qiu, G.; Jia, X.; Cai, J.; Chen, W. Adsorption of Cu<sup>2+</sup> on silica supported by fly ash zeolite. *J. Funct. Mater.* **2019**, *50*, 3152–3158, (in Chinese with English abstract).
28. Purna Chandra Rao, G.P.C.; Satyaveni, S.; Ramesh, A.; Seshiah, K.; Murthy, K.S.N.; Choudary, N.V. Sorption of cadmium and zinc from aqueous solutions by zeolite 4A, zeolite 13X and bentonite. *J. Environ. Manag.* **2006**, *81*, 265–272. [[CrossRef](#)] [[PubMed](#)]
29. Wang, R.; Xin, L.; Li, J.; Chang, H.; Zhang, G. Adsorption of nitrate nitrogen by peanut shell biochar. *J. Agro-Environ. Sci.* **2016**, *35*, 1727–1734, (in Chinese with English abstract).
30. Li, Z.; Wu, L.; Sun, S.; Gao, J.; Zhang, H.; Zhang, Z.; Wang, Z. Disinfection and removal performance for *Escherichia coli*, toxic heavy metals and arsenic by wood vinegar-modified zeolite. *Ecotoxicol. Environ. Saf.* **2019**, *174*, 129–136. [[CrossRef](#)]
31. Li, M.; Zhu, X.; Zhu, F.; Ren, G.; Cao, G.; Song, L. Application of modified zeolite for ammonium removal from drinking water. *Desalination* **2011**, *271*, 295–300. [[CrossRef](#)]
32. Ptáček, P.; Kubátová, D.; Havlica, J.; Brandštetr, J.; Šoukal, F.; Opravil, T. The non-isothermal kinetic analysis of the thermal decomposition of kaolinite by thermogravimetric analysis. *Powder Technol.* **2010**, *204*, 222–227. [[CrossRef](#)]
33. Li, L.X.; Zhang, Y.M.; Zhang, Y.F.; Sun, J.M.; Hao, Z.F. The thermal activation process of coal gangue selected from Zhungeer in China. *J. Therm. Anal. Calorim.* **2016**, *126*, 1559–1566. [[CrossRef](#)]
34. Ates, A.; Hardacre, C. The effect of various treatment conditions on natural zeolites: Ion exchange, acidic, thermal and steam treatments. *J. Colloid Interface Sci.* **2012**, *372*, 130–140. [[CrossRef](#)] [[PubMed](#)]

35. Cardoso, M.J.B.; Rosas, D.D.O.; Lau, L.Y. Surface P and Al distribution in P-modified ZSM-5 zeolites. *Adsorption* **2005**, *11*, 577–580. [[CrossRef](#)]
36. Murayama, N.; Yamamoto, H.; Shibata, J. Mechanism of zeolite synthesis from coal fly ash by alkali hydrothermal reaction. *Int. J. Miner. Process.* **2002**, *64*, 1–17. [[CrossRef](#)]
37. Le van Mao, R.; Lu, L.; Vu, N.T.; Zhao, Q.; Yan, H.T.; Al-Yassir, N. Silica nanoboxes from alumina rich zeolites: Thermal and chemical stability of the monomodal and bimodal materials. *Catal. Lett.* **2007**, *114*, 129–134. [[CrossRef](#)]
38. Tang, X.; Liu, J.; Shang, H.; Wu, L.; Yang, J. Gas diffusion and adsorption capacity enhancement via ultrasonic pretreatment for hydrothermal synthesis of K-KFI zeolite with nano/micro-scale crystals. *Micropor. Mesopor. Mater.* **2020**, *297*, 110036. [[CrossRef](#)]
39. Shen, Y.; Jiao, S.; Ma, Z.; Lin, H.; Gao, W.; Chen, J. Humic acid-modified bentonite composite material enhances urea-nitrogen use efficiency. *Chemosphere* **2020**, *255*, 126976. [[CrossRef](#)]
40. Cheung, W.H.; Szeto, Y.S.; McKay, G. Intraparticle diffusion processes during acid dye adsorption onto chitosan. *Bioresour. Technol.* **2007**, *98*, 2897–2904. [[CrossRef](#)]
41. Yang, T.T.; Xu, Y.M.; Huang, Q.Q.; Sun, Y.B.; Liang, X.F.; Wang, L.; Qin, X.; Zhao, L.J. Adsorption characteristics and the removal mechanism of two novel Fe-Zn composite modified biochar for Cd (II) in water. *Bioresour. Technol.* **2021**, *333*, 125078. [[CrossRef](#)]
42. Kang, X.; Geng, N.; Li, Y.; Li, X.; Yu, J.; Gao, S.; Wang, H.; Pan, H.; Yang, Q.; Zhuge, Y.; et al. Treatment of cadmium and zinc-contaminated water systems using modified biochar: Contaminant uptake, adsorption ability, and mechanism. *Bioresour. Technol.* **2022**, *363*, 127817. [[CrossRef](#)]
43. Belova, T.P. Adsorption of heavy metal ions (Cu<sup>2+</sup>, Ni<sup>2+</sup>, Co<sup>2+</sup> and Fe<sup>2+</sup>) from aqueous solutions by natural zeolite. *Heliyon* **2019**, *5*, e02320. [[CrossRef](#)] [[PubMed](#)]
44. Jiménez-Castañeda, M.E.; Medina, D.I. Use of surfactant-modified zeolites and clays for the removal of heavy metals from water. *Water* **2017**, *9*, 235. [[CrossRef](#)]
45. Choi, H.J.; Yu, S.W.; Kim, K.H. Efficient use of Mg-modified zeolite in the treatment of aqueous solution contaminated with heavy metal toxic ions. *J. Taiwan Inst. Chem. Eng.* **2016**, *63*, 482–489. [[CrossRef](#)]
46. Qiu, M.; He, C. Efficient removal of heavy metal ions by forward osmosis membrane with a polydopamine modified zeolitic imidazolate framework incorporated selective layer. *J. Hazard. Mater.* **2019**, *367*, 339–347. [[CrossRef](#)] [[PubMed](#)]
47. Han, R.; Zou, W.; Wang, Y.; Zhu, L. Removal of uranium(VI) from aqueous solutions by manganese oxide coated zeolite: Discussion of adsorption isotherms and pH effect. *J. Environ. Radioact.* **2007**, *93*, 127–143. [[CrossRef](#)]
48. Wu, F.C.; Tseng, R.L.; Juang, R.S. Initial behavior of intraparticle diffusion model used in the description of adsorption kinetics. *Chem. Eng. J.* **2009**, *153*, 1–8. [[CrossRef](#)]
49. Peng, Z.; Lin, X.; Zhang, Y.; Hu, Z.; Yang, X.; Chen, C.; Chen, H.; Li, Y.; Wang, J. Removal of cadmium from wastewater by magnetic zeolite synthesized from natural, low-grade molybdenum. *Sci. Total Environ.* **2021**, *772*, 145355. [[CrossRef](#)]
50. Al-aAnber, M.; Al-Anber, Z.A. Utilization of natural zeolite as ion-exchange and sorbent material in the removal of iron. *Desalination* **2008**, *225*, 70–81. [[CrossRef](#)]
51. Wang, T.; Liu, W.; Xiong, L.; Xu, N.; Ni, J. Influence of pH, ionic strength and humic acid on competitive adsorption of Pb (II), Cd (II) and Cr (III) onto titanate nanotubes. *Chem. Eng. J.* **2013**, *215–216*, 366–374. [[CrossRef](#)]
52. Jiang, S.; Huang, L.; Nguyen, T.A.H.; Ok, Y.S.; Rudolph, V.; Yang, H.; Zhang, D. Copper and zinc adsorption by softwood and hardwood biochars under elevated sulphate-induced salinity and acidic pH conditions. *Chemosphere* **2016**, *142*, 64–71. [[CrossRef](#)]
53. Moreno, N.; Querol, X.; Ayora, C.; Pereira, C.F.; Janssen-Jurkovicová, M. Utilization of zeolites synthesized from coal fly ash for the purification of acid mine waters. *Environ. Sci. Technol.* **2001**, *35*, 3526–3534. [[CrossRef](#)] [[PubMed](#)]

**Disclaimer/Publisher’s Note:** The statements, opinions and data contained in all publications are solely those of the individual author(s) and contributor(s) and not of MDPI and/or the editor(s). MDPI and/or the editor(s) disclaim responsibility for any injury to people or property resulting from any ideas, methods, instructions or products referred to in the content.